IEEE Transactions on Power Apparatus and Systems, Vol. PAS-96, no. 4, July/August 1977

STEADY-STATE ANALYSIS OF A CURRENT SOURCE INVERTER/RELUCTANCE MOTOR DRIVE PART II: EXPERIMENTAL AND ANALYTICAL RESULTS

C. M. Ong
Purdue University
West Lafayette, IN

T. A. Lipo
General Electric Co.
Schenectady, NY

SUMMARY

The steady-state solution of a reluctance motor supplied from a current source inverter, derived in Part I, is compared with both experimental and simulation results. The calculated results from closed form expressions for instantaneous motor line voltage and current are compared to results obtained from experiment. Correlation of internal machine variables is obtained using simulation techniques. Effects of current source operation on important design parameters such as average and pulsating components of electromagnetic torque, stator and rotor copper losses are calculated and discussed.

INTRODUCTION

In a companion paper [1], the closed-form, time domain solutions have been derived which describe the steady-state behavior of a synchronous-reluctance motor operating from a current source inverter. In this paper, the results of the analysis are compared to laboratory test data. Further comparison is obtained with data from an analog computer simulation in which the inverter and motor are represented in detail. Since reluctance motor drives are typically used in precise speed, high duty factor applications, system parameters such as torque pulsations and motor heating assume considerable importance. In this paper these and other important operating characteristics of this new type of ac motor drive are displayed and compared to test results.

COMPARISON OF TESTED AND COMPUTED RESULTS

In order to verify the analysis technique presented in Part I, the solutions that have been developed were evaluated by means of a digital computer and compared to the tested results from an actual system. For purposes of comparison, the reluctance machine used in this study was a 10 HP, 220V, 4 pole, 60 Hz, delta-connected machine. The motor windings were reconnected in wye to eliminate possible circulating currents so that rated rms phase voltage was 220V. The per-phase parameters measured by means of a locked rotor test at rated frequency are: stator resistance and leakage reactance; $r_s = 0.215\Omega$, $x_{\ell s} = 0.596\Omega$, d-axis rotor resistance and leakage reactance; $r'_{dr} = 0.18\Omega$, $x'_{\ell dr} = 0.11\Omega$, and q-axis rotor resistance and leakage reactance, $r'_{qr} = 0.365\Omega$, $x'_{\ell qr} = 1.34\Omega$. The magnetizing reactances for the test machine were obtained from a non-load test by driving the reluctance machine with a synchronous motor and shifting the relative phase of the voltages applied to the two machines by means of a rotary transformer [2]. The measured saturation curves in the d- and q-axes of the reluctance machine are shown in Fig. 1. Both short-circuit and no-load tests were performed with sinusoidal excitation.

When stator current rather than voltage is the independent variable, it is apparent that the saturation within the machine will vary widely from no-load to the pull-out condition. It is therefore, important that saturation be properly taken into account. Although not explicitly considered in the analysis of Part I, the effect of saturation can be readily incorporated into the solution using the technique described by Williamson [2].

This paper recommended and approved by the Rotating Machinery Committee of the IEEE Power Engineering Society. This paper was presented at the 1975 Tenth Annual Meeting of the IEEE IAS and was published in the IEEE Conference Record of the 1975 (75 CHO 999-3IA).

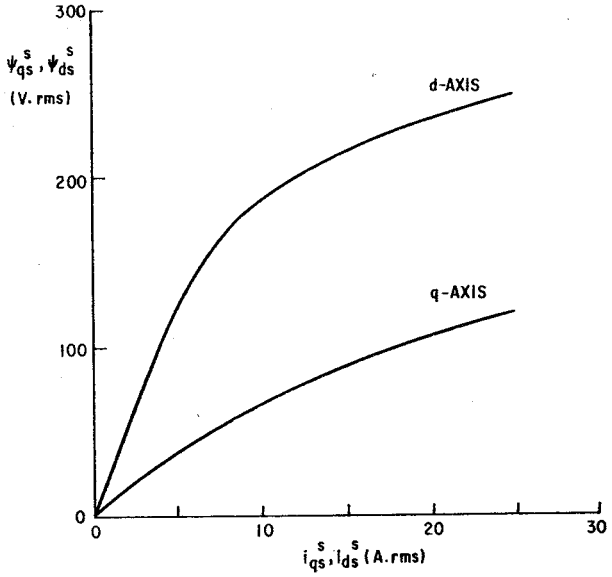

Fig. 1. Measured d- and q- axis saturation curves.

Fig. 2. Steady-State phase voltage and current for the condition $I_R = 25$ A., $f_e = 30$ Hz., $T_L = 28.5$ N.m. Tested results from experimental system. Scale; v_{ac} – 200 V/div. i_{as} – 20 A./div.

Figures 2 and 3 show a comparison of the analytical results with data obtained from an actual system. At the operating point shown, the motor was excited with 30 Hz. The dc link current adjusted to 25A and the reluctance motor loaded to 28.5 Nm. Comparing Fig. 2 to Fig. 3 it can be noted that the line voltage is sinusoidal as predicted and its amplitude and phase relative to the quasi-square line current compares favorably with the calculated result.

In general, only stator terminal voltage and current can be measured conveniently in the laboratory so that comparison with experiment is limited. As a means to provide further correlation the complete inverter with associated commutation circuit and reluctance motor was simulated on the hybrid computer. Traces obtained from the simulation are given in Fig. 4. Comparison with the calculated results, Fig. 3, indicates favorable correlation of rotor currents and electromagnetic torque as well as for stator variables. However, a precise correlation is not pos-

sible since the commutation time for the system parameters and operating point chosen is becoming appreciable. In practice the dc link inductor cannot be made arbitrarily large so a ripple component of dc link current appears in the experimental system. However, the filter inductance can be made sufficiently large so that the consequences of this effect can be assumed to be negligible.

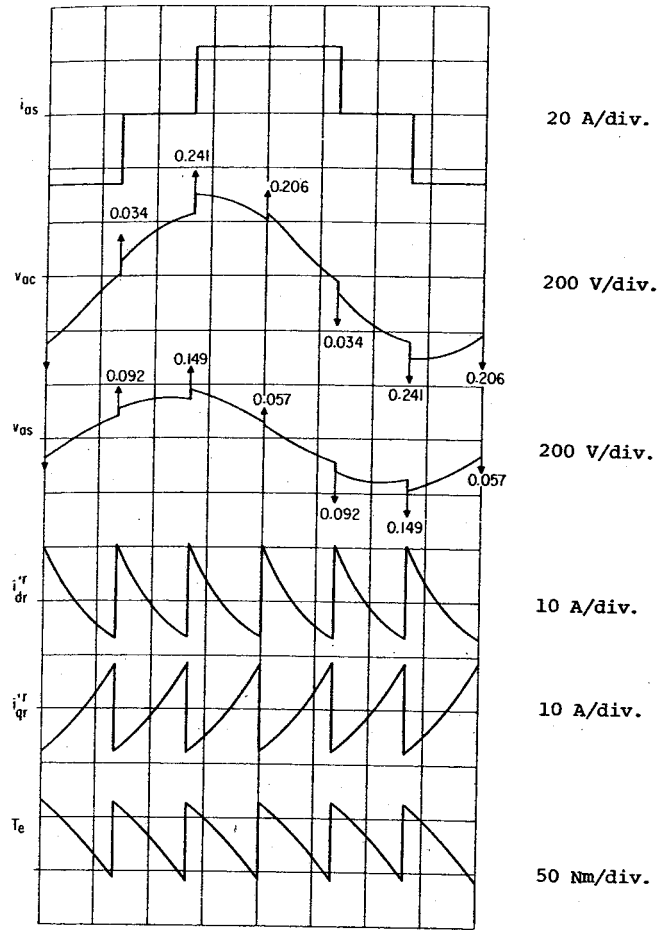

Fig. 3. Steady-state motor variables for the condition I_R = 25 A., f_e = 30 Hz., T_L = 28.5 N.m. Calculated results from closed form solution.

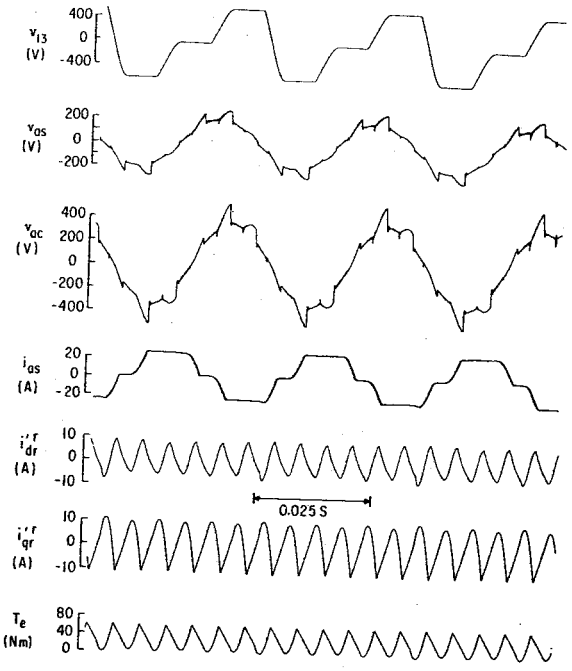

Fig. 4. Steady-state motor variables for the condition I_R = 25 A., f_e = 30 Hz., T_L = 28.5 N.m. Detailed hybrid computer simulation including the effects of inverter parameters and finite rotor inertia. Voltage v_{13} is the inverter commutation capacitor voltage.

WAVEFORMS

Since commutation time has been assumed negligibly small, the calculated waveforms show abrupt changes (discontinuities) at the switching instants of the inverter. The stator voltages during commutation are represented by impulses with corresponding magnitude ('strength') as shown. The strength of these voltage impulses which ride on the stator voltages can be calculated from the first term of Eqs. 57 and 58 in Part I. In practice, the commutation interval of the inverter with a reluctance machine load are of finite duration and consequently the rates of change of the variables are less abrupt. A profile of the stator voltage variation during commutation provides useful design information of the voltage stresses on the SCR devices. It is recognized that the expression for the voltage impulse strength falls short of this requirement. However, commutation time can be estimated if the commutation capacitance is known so that it is possible to obtain the peak voltage as a function of current excitation, transient reactance and load angle by equating the integral of the volt-second area under an approximate voltage pulse to the voltage impulse strength.

During commutation the change in magnetic field energy of the machine given by Eqs. 62 and 63 (Part I) is transferred to the inverter and temporarily stored as electrostatic energy in the commutating capacitor. The commutation capacitor thus receives a boost of voltage during commutation. The voltage stresses on the SCR devices are related to the capacitor voltages and the line voltages of the machine. To minimize the voltage stresses on the SCR devices, commutation capacitance should be as large as possible and the change in magnetic field energy which occurs during commutation should be reduced. Equations 62 and 63 relate the change of magnetic field energy to current excitation, machine transient reactances and load angle. With a given load, voltage stresses on the thyristors will be minimized if the current excitation is kept as small as possible. Overexcitation not only results in higher voltage stresses but also higher torque pulsation and higher losses as is apparent from the expressions in Part I, Appendix II.

Examination of Figs. 3 and 4 indicate that even for steady-state operation, induced harmonic currents flow in the rotor windings. Since the resultant armature MMF produced by idealized phase currents switches around by 60° at the instant of each inverter switching, the basic switching frequency of the stator MMF corresponds to that of the inverter. However, the MMF does not rotate with a uniform angular speed as does the rotor. Between switching instants the stator MMF is stationary in space and the rotor rotates with uniform synchronous speed and as a result of the relative motion rotor currents are induced. As expected, these rotor currents have zero mean-value. The interaction of harmonic rotor currents and the air gap flux produces harmonic torques. It is an interesting result of this analysis that the harmonic torque component always has a mean value which is in a fixed proportion to the nominal reluctance torque resulting from the fundamental component of stator current.

DISCUSSION OF STEADY-STATE PERFORMANCE

In order to establish a basis for comparison, another machine was selected more typical of those machines used for high horsepower applications. For convenience, per unit parameters were employed to

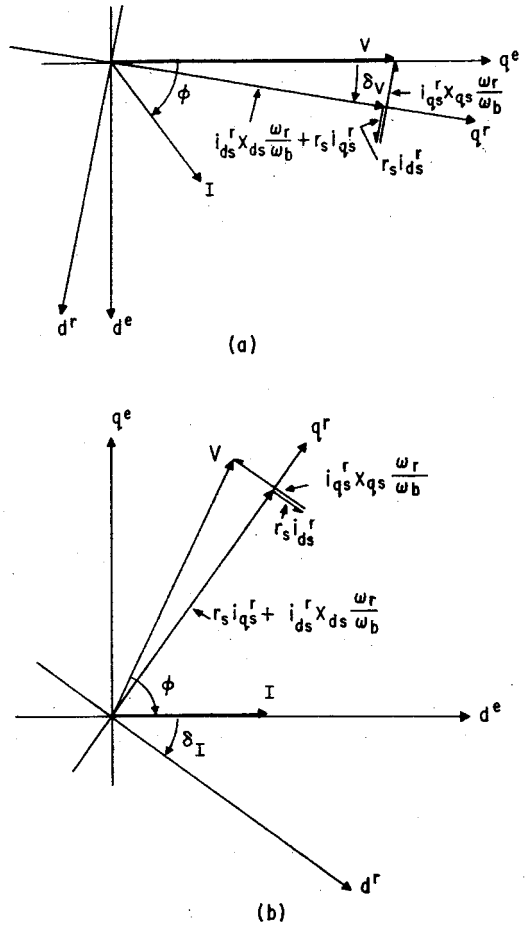

Fig. 5. Reluctance motor vector diagrams. a) voltage source, b) current source.

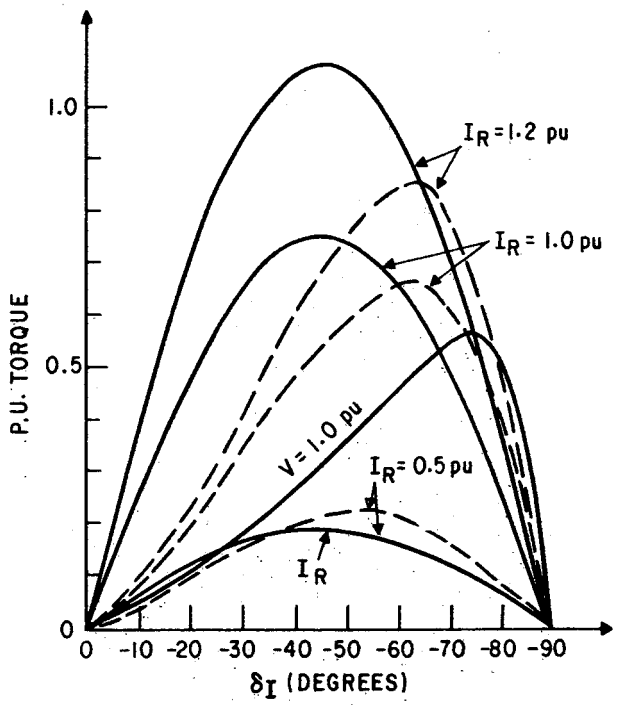

Fig. 6. Average torque vs. load angle δ_I. Solid (dashed) line, saturation neglected (included).

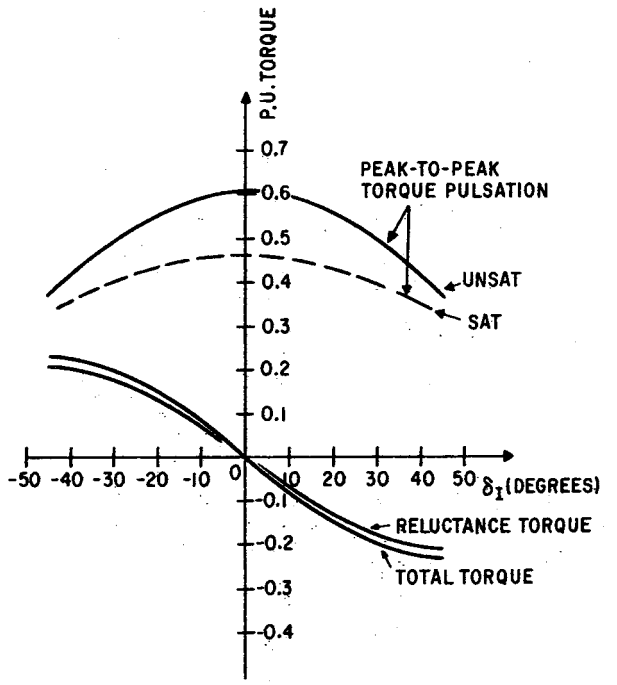

Fig. 7. Average and pulsating components of torque vs. δ_I, I_R = 0.5 pu.

enable direct use of the results of Part I. In per unit, the parameters for this machine are $r_s = 0.045$, $r'_{dr} = 0.030$, $r'_{qr} = 0.015$, $x_{\ell s} = 0.1$, $x'_{\ell dr} = 0.1$, $x'_{\ell qr} = 0.1$, x_{ds} (unsat) = 2.1, x_{qs} (unsat) = 0.6 pu. Since saturation is an important consideration in this type of drive, the curves similar to those plotted in Fig. 1 were employed to account for saturation.

It is of interest to compare the torque-angle characteristics of the synchronous-reluctance machine when fed from a sine wave current source and from a sine wave voltage source. For this purpose, it is convenient to employ the vector diagram shown in Fig. 5. This figure also serves to emphasize the difference between the torque angle for constant current δ_I and the conventional torque angle δ valid for a constant voltage source (herein denoted as δ_V). The average torque vs. δ_I curves for various operating current and voltage magnitudes are given in Fig. 6 respectively both for the case of unsaturated and saturated machines. The effect of saturation clearly reduces the torque available at small load angles (high flux condition). Note also that saturation shifts the point of pullout to a higher value of δ_I. Saturation also tends to reduce the synchronizing torque coefficient, $\partial P/\partial\delta$, particularly for low torque angles. However, it is evident from these figures that regardless of saturation the current-fed machine has higher synchronizing torque coefficient over the practical operating range of load angle.

The nature of torque production in the machine is further clarified by Fig. 7. The average component of torque denoted as reluctance torque is that portion resulting from the fundamental component of stator current. The total torque includes the effect of the harmonics on torque production. Note that harmonic components of current tend to improve the net torque capability of the machine, in direct contrast to the case with a conventional voltage source inverter. [3] Also from Fig. 7 it can be observed that the pulsating part of the harmonic torque is highest at no-load and gradually decreases with higher loading in both the generating and motoring regions. For purposes of comparison, the pulsating torques with and without saturation effects, have been plotted. It can be noted that effects of saturation reduce the pulsating torques especially at light loads. Referring to Eq. 64 in Part I, it can be observed that torque pulsation is a function of both rotor saliency and dc link current. A decrease in rotor saliency tends to reduce the torque pulsation. Also, the pulsating torque components are sensitive to

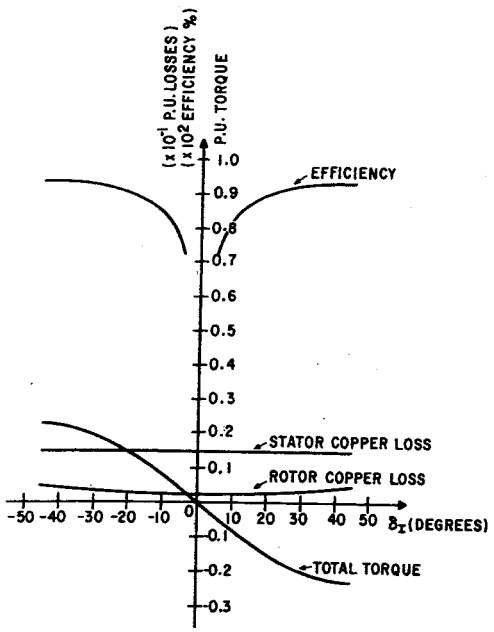

Fig. 8. Reluctance motor performance characteristics operating from a current source inverter.

changes in dc link current since this quantity appears in Eq. 64 as a squared term. This behavior emphasizes the importance of keeping the current excitation level optimum for a particular loading since overexcitation will result in both higher torque pulsations and in higher losses.

The general performance characteristics of the machine with current source operation have been plotted in Fig. 8. Excluding iron and rotational losses, the efficiency of the reluctance machine in the motoring and generating regions of operation can be computed from the total output and the copper losses in the rotor and stator circuits. Saturation has the effect of reducing efficiency. It can be seen from Fig. 8 that for operation with constant current input, stator copper losses remain constant for varying load angle, and the rotor copper loss increases with higher loading. An unexpected but significant result of this study was the determination that for constant load and input current, both stator and rotor copper losses as well as the average and pulsating torque components are independent of operating frequency. This result is again in direct contrast to the results obtained for a voltage inverter source. [3] In practice, of course, both stator and rotor resistances as well as iron loss will be somewhat frequency dependent resulting in a slight increase in losses as frequency increases.

CONCLUSION

In this two-part paper, the complete steady-state solution of a reluctance motor supplied for a current-source inverter has been obtained. Since the solution is expressed as an explicit function of time, the effects of all motor parameters on any variable of interest can be readily observed. Since the solution is in closed form, computing time required to obtain the desired solutions is minimal.

Reluctance motor drives serve a large portion of the present-day static drive market. It appears that application of current source inverters to this class of ac motor drive will be inevitable. Hence, the results of these papers should prove a welcome aid to the engineer engaged in a specific design application.

ACKNOWLEDGMENTS

The work summarized in this paper was sponsored in part by an NSF grant. The computer studies were performed at the Purdue University Hybrid Computer Laboratory using equipment provided in part by NSF. The authors wish to thank Mr. G. E. Gareis for his assistance.

REFERENCES

[1] C. M. Ong and T. A. Lipo, "Steady-state analysis of a current source inverter/reluctance motor drive, Part I: Analysis", *IEEE Transactions on Power Apparatus and Systems*, this issue.

[2] A. C. Williamson, "Calculation of saturation effects in segmented-rotor reluctance machines", *Proc. IEE*, Vol. 121, No. 10, Oct. 1974, pp. 1127-1133.

[3] K. Heumann and K. G. Jordan, "Effects of voltage and current upper harmonics on the operation of induction motors", *AEG Mitt.*, Vol. 54, No. 1/2, 1964, pp. 117-122, (In German).